

Published in final edited form as:

Circulation. 2014 July 29; 130(5): 431–441. doi:10.1161/CIRCULATIONAHA.113.006720.

PCSK9 Promotes Intestinal Overproduction of Triglyceride-Rich Apolipoprotein-B Lipoproteins Through Both LDL-Receptor Dependent and Independent Mechanisms

Shirya Rashid, Ph.D.¹, Hagai Tavori, Ph.D.^{2,3}, Patrick E. Brown, Ph.D.⁴, MacRae F. Linton, M.D.², Jane He, B.Sc.², Ilaria Giunzioni, M.Sc.², and Sergio Fazio, M.D., Ph.D.²

¹Department of Pharmacology, Dalhousie University, Halifax, Nova Scotia and Saint John, New Brunswick, Canada

²Department of Medicine, Section of Cardiovascular Disease Prevention, Vanderbilt University, Nashville, TN

³Oregon Health and Science University, Portland, OR

⁴Department of Biostatistics, Faculty of Medicine, University of Toronto and Cancer Care Ontario, Canada

Abstract

Background—Proprotein convertase subtilisin kexin type 9 (PCSK9) promotes the degradation of the low-density lipoprotein receptor (LDLR), and its deficiency in humans results in low plasma LDL-cholesterol and protection against coronary heart disease (CHD). Recent evidence indicates that PCSK9 also modulates the metabolism of triglyceride-rich apolipoprotein B (apoB) lipoproteins (TRL), another important CHD risk factor. Here we studied effects of physiological levels of PCSK9 on intestinal TRL production and elucidated for the first time the cellular and molecular mechanisms involved.

Methods and Results—Treatment of human enterocytes (CaCo-2 cells) with recombinant human PCSK9 (10 µg/mL, 24 hours) increased cellular and secreted apoB48 and apoB100 by 40–55% each ($p < 0.01$ vs. untreated cells), whereas acute deletion of *PCSK9* expression reversed this effect. PCSK9 stimulation of apoB was due to: (1) a 1.5-fold increase in apoB mRNA ($p < 0.01$); and (2) enhanced apoB protein stability through both LDLR-dependent and LDLR-independent mechanisms. PCSK9 decreased LDLR protein ($p < 0.01$) and increased cellular apoB stability via activation of microsomal triglyceride transfer protein (MTP). PCSK9 also increased levels of the lipid-generating enzymes *FAS*, *SCD* and *DGAT2* ($p < 0.05$). In mice, human PCSK9 at physiologic levels increased intestinal MTP levels and activity regardless of LDLR expression.

Conclusions—PCSK9 markedly increases intestinal TRL apoB production through mechanisms mediated in part by transcriptional effects on apoB, MTP and lipogenic genes, and in part by post-

Correspondence: Shirya Rashid, PhD, Associate Professor, Department of Pharmacology, Faculty of Medicine, Dalhousie University, Dalhousie Medicine New Brunswick (DMNB), 100 Tucker Park Road, PO Box 5050, Saint John NB E2L 4L5 Canada, Phone: 506-636-6972, Fax: 506-636-6001, shirya.rashid@Dal.ca.

Conflict of Interest Disclosures: None.

transcriptional effects on the LDLR and MTP. These findings indicate that targeted PCSK9-based therapies may also be effective in the management of postprandial hypertriglyceridemia.

Keywords

lipids and lipoprotein metabolism; apolipoproteins; risk factors; pathophysiology; molecular biology

Introduction

Proprotein convertase subtilisin/kexin type 9 (PCSK9) is a secreted serine protease that plays an important role in atherosclerotic coronary heart disease (CHD) development in humans. Gain-of-function mutations in PCSK9 are associated with autosomal dominant hypercholesterolemia and sharply increased risk of coronary artery disease (CAD)¹, while loss-of-function mutations are accompanied by remarkably large reductions in CHD risk². These findings have generated intense investigations in PCSK9 biology, which have attributed potential pro-atherosclerotic properties to PCSK9, linked to its effect on serum low-density lipoprotein cholesterol (LDL-C) levels³, raised by PCSK9-mediated degradation of hepatic LDL receptors (LDLR)⁴, which then causes a secondary increase in plasma PCSK9 levels⁵.

It has recently emerged, however, that PCSK9 also affects the metabolism of triglyceride-rich, apolipoprotein (apo) B-containing lipoproteins (TRL)^{5,6}. Triglyceride and apoB levels significantly and independently associate with CHD risk⁷. Furthermore, TRL remnant particles drive cholesterol accumulation in arterial macrophages and cause progression of coronary artery disease⁸.

Relatively few investigations have targeted the regulatory role of PCSK9 on TRL. Most of them have focused on the effect of PCSK9 on TRL metabolism at the hepatic level and have identified PCSK9 as a trigger of TRL production^{5,6,9}. The intestine is another major source of TRL, accounting for a significant portion of plasma lipids in the form of postprandial chylomicrons, with apoB48 as their characteristic apolipoprotein^{10,11}. It must be noted that PCSK9 expression in the intestine is quantitatively second only to hepatic expression¹².

Here we investigated for the first time the comprehensive cellular, molecular and physiologic mechanisms through which PCSK9 causes intestinal TRL overproduction. Our results reveal that PCSK9 regulation of intestinal TRL metabolism is imparted at both transcriptional (lipid and apoprotein biosynthesis) and post-transcriptional levels (TRL assembly). Furthermore, we show that the effects of human PCSK9 on intestinal TRL apoB production are mediated through both LDLR dependent and independent means, and involve MTP. Finally, we showed that acute PCSK9 knockdown substantially reduces enterocyte TRL production via down-regulation of key protein mediators of the cellular TRL production pathway.

Methods

Cell Culture

Cultured CaCo-2 cells were obtained from American Type Culture Collection (ATCC, VA). CaCo-2 cells were first grown for 3 days in EMEM specialty medium (ATCC, VA) in 20% FBS supplemented with 1% penicillin-streptomycin, at 37°C, 5% CO₂, until they reached 80–90% confluence. Induction of cell polarization is necessary for CaCo-2 cells to resemble human intestinal enterocytes *in vivo*. To induce polarization, CaCo-2 cells were maintained in culture in 10% FBS-DMEM for 14 days in specialized, collagen-treated transwell plates with 0.4 µm pore size polycarbonate filters (CoStar, DC).

Unless otherwise indicated, all studies were performed at least three times. Optimally polarized confluent CaCo-2 cells in 1% FBS-DMEM were treated for 24 hours with recombinant human PCSK9 (R&D Systems, MN) reconstituted in Millipore H₂O. PCSK9 was mostly used at the concentration of 10 µg/mL for 24 hours¹³, although many experiments included different doses (0, 5, 7.5, 10 and 12 µg/mL) and different times (0, 2, 4, 8, 12, and 24 hours).

Mice

C57BL/6 (Wild-type, WT) and LDLR^{-/-} mice were purchased from the Jackson Laboratories (The Jackson Laboratory, ME) and housed at Vanderbilt University Medical Center. hPCSK9 transgenic mice were generated in our laboratory as previously described¹⁴. All animal experiments were carried out in compliance with National Institutes of Health guidelines and were approved by the Institutional Animal Care and Use Committee of Vanderbilt University.

PCSK9 siRNA Studies

Four small interfering ribonucleic acid vectors (siRNAs) targeting human PCSK9, (Qiagen, MD), were transfected into CaCo-2 cells at a final concentration of 15 nmol/L, using HiPerFect transfection reagent (Qiagen, MD) at 0.5% final volume¹⁵. The siRNA that produced the maximum decrease in PCSK9 mRNA and protein expression (70% mRNA knockdown 48 hours post-transfection) was chosen for further experiments. As a negative control, CaCo-2 cells were transfected with a scrambled siRNA control vector containing a nonsense mRNA sequence (Qiagen, MD). As a positive control, CaCo-2 cells were transfected with siRNA targeting and silencing the constitutively expressed GAPDH gene.

Immunoprecipitation and Western Blots

Cell lysates, collected with RIPA buffer (50 mM Tris, 150 mM sodium chloride, 1% NP-40, 12 mM sodium deoxycholate, 3.5 mM SDS, pH 7.4) and protease inhibitor cocktail (Roche Diagnostics, QC), and media, were immunoprecipitated for apoB48, apoB100, LDLR, MTP, NPC1L1, PCSK9, GAPDH, beta-actin and albumin, using Catch-and-Release immunoprecipitation columns and kits (Millipore, MA)¹⁶. Immunoprecipitates were subjected to sodium dodecyl sulfate polyacrylamide gel electrophoresis (SDS-PAGE), transferred onto nitrocellulose membranes (BioRad, CA) and immunoblotted using antibodies against apoB48 and apoB100 (human) (Santa Cruz, CA), PCSK9 (Cayman

Chemicals, MI), LDLR (Fitzgerald International, CA), MTP (Santa Cruz, CA), Niemann-Pick C1 like 1 (NPC1L1) (Santa Cruz, CA), GAPDH (Sigma, MO), beta-actin (Sigma-Aldrich, MO) and albumin (Santa Cruz, CA). Horseradish peroxidase–conjugated antibodies (BioRad, CA) were used as secondary antibodies. Immunoreactive bands were visualized with a chemiluminescence kit (PerkinElmer Life Sciences, MA). The blots were exposed to KODAK Biomax films, and the signal was quantified by densitometry using Quantity One version 4.6.7. software (Bio Rad, CA).

Samples of proximal small intestine and large intestine were lysed with modified RIPA Buffer (Sigma, MO). Samples (50µg) were loaded onto NuPage 4% to 12% Bis-Tris gels (Life Technologies, CA) for electrophoresis and the size-separated proteins were transferred to nitrocellulose membranes. Primary antibodies toward MTP (a kind gift of Prof. Larry Swift from the Vanderbilt University), β-actin (Abcam, MA) and GAPDH (Novus biological, CO) and horseradish peroxidase–conjugated secondary antibodies (Sigma, MO) were used to detect target proteins. Signal was detected by use of a mixture of luminol, p-coumaric acid, and hydrogen peroxide in 100 mmol/L Tris (pH 8.5). Intensity quantification of the bands was obtained with ImageJ software and normalized to β-actin or GAPDH.

Semi-Quantitative PCR

Total RNA was isolated from the proximal part of the small intestine and distal part of the large intestine using TRIzol reagent (Invitrogen Life Technologies, CA) and processed for reverse transcription with the iSCRIPT cDNA synthesis (Biorad). cDNA was amplified using Platinum PCR MasterMix™ (Invitrogen Life Technologies, CA) and primers for MTP (forward primer: TGGTCAGGAAGCTGTGTCAG and reverse primer: GAAGCAAGGCATTCTTCAGG) and β-actin (forward primer: AGGGAAATCGTGCGTGACAT and reverse primer: CGTTGCCAATAGTGATGACC) and loaded onto a 4% agarose gel.

Real-Time Quantitative Reverse-Transcriptase (RT)-PCR Analysis

Total RNA was isolated from cell lysates (RNeasy Mini Kit, Qiagen, MD) and used as templates for cDNA synthesis (QuantiTech Reverse Transcription Kit, Qiagen, MD). Quantitative real-time RT-PCR was performed using an Applied Biosystems 7300 Real Time PCR system (Carlsbad, CA), according to the manufacturer's instructions, and with the SYBR green master kit (Qiagen, MD)¹⁶. Primers for RT-PCR succinate dehydrogenase (*SDH*), *APOB*, *MTP*, *SREBP1*, *SREBP2*, HMG-CoA reductase, HMG-CoA synthase, squalene synthase (*SS*), *LDLR*, *PCSK9*, fatty acid synthase (*FAS*), stearoyl-CoA desaturase (*SCD*), diglyceride acyltransferase 1 (*DGAT1*) and *DGAT2* were purchased (the proprietary sequences are not available) (Qiagen, MD). The values reported for each mRNA were corrected to *SDH* mRNA values. Relative quantifications of MTP mRNA from small and large intestine samples was performed with the ABI Prism 7700 Sequence Detection System (Applied Biosystems Life Technologies, CA) using TaqMan gene expression assays (Applied Biosystems Life Technologies, CA). Expression levels were calculated using the CT method and normalized to 18S rRNA levels.

Oil-Red-O and Hematoxylin Staining

Cells were stained with Oil-Red-O to examine the total amount of neutral lipid accumulation in the cells, as previously described¹⁶.

Cell Viability

Cell viability was determined using 0.4% trypan blue (Sigma-Aldrich, ON) staining and calculated using the following formula:

$$\% \text{ Cell Viability} = \frac{\text{Number of Unstained (Living) Cells}}{\text{Total Number of Cells}} \times 100^{16}$$

Microsomal Triglyceride Transfer Protein (MTP) Activity Assay

Cell monolayers were washed twice with cold PBS and once with 5 mL of buffer (1 mM Tris-HCl, pH 7.6, 1 mM EGTA and 1 mM MgCl₂) at 4 °C. Cells were then incubated for 2 minutes at room temperature in 5 mL of cold buffer. The buffer was aspirated and 0.5 mL of the same buffer was added to cells. Small pieces (50–70 mg) of proximal small intestine were collected and homogenized in 0.5 ml of the same buffer. Cells and tissues were scraped, collected, vortexed and centrifuged (SW55 Ti rotor, 50,000 rpm, 10 °C, 1 hour or TLA 120.2 rotor, 90,000 rpm, 4 °C, 1 h – depending on sample size) and supernatants were tested for MTP activity using a kit (Chylos Inc., NY) as previously described¹⁷. The triglyceride transfer activity of MTP was measured as % lipid transfer/h/mg protein.

Statistical Analyses

Data (Figures 1–4) were analyzed using Wilcoxon rank sum tests and a Bonferroni correction was applied for multiple pairwise comparisons. The *in vivo* data (Figure 5 and Figure 6 and Supplemental Figures 1 and 2) were analyzed using t-tests or ANOVA, as appropriate, with the Bonferroni test for post-hoc comparisons. All results are presented as means ± SEM. Asterisks indicate statistically significant differences (*P<0.05 and **P<0.01) compared with respective controls.

Results

PCSK9 Directly Stimulates ApoB Cellular Protein Expression and Secretion in Human Enterocytes

Confluent, polarized CaCo-2 cells in 1% FBS-DMEM were treated for 24 hours with recombinant human PCSK9. Of note, CaCo-2 cells secreted negligible amounts of human PCSK9 relative to the 10 µg/mL concentration of recombinant PCSK9 added to the media during the experiments. The identity of recombinant human PCSK9 was confirmed by immunoblot (Figure 1A).

The addition of physiologic levels of human PCSK9 (10 µg/mL)¹⁸ to optimally polarized human enterocytes (CaCo-2 cells) resulted in an approximately 50% increase in apoB cellular protein expression and a similar increase in secreted apoB compared with untreated CaCo-2 cells (Figures 1B and 1C). This stimulatory effect of PCSK9 was rapid, occurring at 24 hours post-treatment, and prolonged, lasting at least 48 hours.

PCSK9 treatment (10 µg/mL, 24 hours) markedly stimulated enterocyte production and secretion of both apoB48 (Figure 1B) and apoB100 (Figure 1C) proteins. Whereas intestinal human TRL only contain the apoB48 isoform, CaCo-2 cells secrete TRL containing both apoB48 and apoB100¹⁹, allowing us to characterize the effect of PCSK9 on both apoB proteins. We found quantitatively similar stimulatory effects on both forms of apoB.

We next performed dose–response and time-course experiments, to assess enterocyte apoB secretion (Figure 1D.). The maximum stimulatory effect of PCSK9 on both apoB48 and apoB100 secretion was seen with 10 µg/mL of PCSK9, and no further stimulation was obtained with 12.5 µg/mL. Moreover, a significant increase in secreted apoB was observed in PCSK9 treated enterocytes as early as 4 hours after PCSK9 treatment (10 µg/mL), an effect that persisted for 24 hours, the time point at which the maximal cumulative effect of PCSK9 on apoB secretion was observed (Figure 1E.).

Quantification of the Contribution of PCSK9 to Enterocyte ApoB Production

PCSK9 siRNA treatment reduced PCSK9 mRNA levels by 70% ($p < 0.01$) compared with CaCo-2 cells transfected with a scrambled negative control vector. Treatment with the PCSK9 siRNA also caused a 40% reduction in the secretion of both apoB48 and apoB100 (Figure 2).

Stimulation of Enterocyte ApoB Production by PCSK9 Occurs at the Transcriptional Level on Cellular Apolipoprotein and Lipid Biosynthesis

Whether enterocyte apoB production by PCSK9 is regulated at the transcriptional level was assessed via real-time RT-PCR analyses. Our results show a significant 1.5-fold increase in apoB mRNA levels in PCSK9 treated cells (10 µg/mL, 24 hours) (Figure 3A) and a converse 50% decrease in apoB mRNA in cells transfected with PCSK9 siRNA (48 hours) (Figure 3A) compared with control untreated cells, demonstrating the specificity of the apoB mRNA effect by PCSK9.

As intracellular neutral lipids inhibit cellular apoB protein degradation and enhance apoB protein stability²⁰, we determine if an increase in cellular neutral lipids contributes to the enhanced cellular apoB protein expression and secretion with PCSK9. We therefore performed Oil-RedO/hematoxylin staining of CaCo-2 cells. The results showed a clear increase in enterocyte neutral lipid content in PCSK9-treated (10 µg/mL, 24 hours) cells versus control untreated cells (Figure 3B) and also a slight increase in cellular neutral content in enterocytes treated with PCSK9 siRNA (48 hours) (Figure 3C).

To study whether the PCSK9-mediated increase in enterocyte lipid content is attributable to increased cellular *de novo* lipogenesis, we measured expression levels of *SREBP1* (fatty acid and triglyceride synthesis) and *SREBP2* (cholesterol synthesis and uptake) target genes. The results showed that PCSK9 treatment (10 µg/mL, 24 hours) caused a 1.5 to 2-fold increase in mRNA levels of *SREBP1* target genes, such as *FAS*, *SCD*, and *DGAT2* (Figure 3D). There was no change, however, in *SREBP1* or *DGAT1* expression. As well, no differences were observed in the mRNA levels of *SREBP2* or *SREBP2* target genes, *HMGCR*, *HMGCS*, *SS*, *LDLR* or *PCSK9* (Supplementary Table 1).

Treatment with PCSK9 siRNA (48 hours) showed no change in mRNA levels of *SREBP1* or *SREBP1* target genes, with the exception of a slight increase in the expression of *DGAT2* (Figure 3D). Despite no effects on *SREBP2* mRNA levels, PCSK9 siRNA produced significant reductions in *SREBP2* target genes involved in cholesterol biosynthesis, *HMGCR*, *HMGCS* and *SS* (Figure 3E). However, there was no change in *SREBP2* targets involved in cholesterol uptake, *LDLR* and *PCSK9* (Supplementary Table 2).

MTP is crucial for the transfer of neutral lipids to apoB and a key regulator of intracellular apoB degradation and stability²⁰. Enterocytes treated with PCSK9 (10 µg/mL, 24 hours) showed a nearly 2-fold increase in MTP mRNA levels (Figure 3A), whereas PCSK9 siRNA treated enterocytes (48 hours) demonstrated a 20% reduction in MTP mRNA (Figure 3A).

Key Protein Mediators through which PCSK9 Stimulates Enterocyte ApoB Production

Treatment of enterocytes with PCSK9 (10 µg/mL, 24 hours) markedly (2.5-fold) increased cellular levels of the active, 62-kDa form of PCSK9. This suggests that following entry into the cell, a substantial amount of exogenous PCSK9 does not undergo lysosomal degradation (Figure 4A).

PCSK9 reduced enterocyte LDLR protein expression by 50%, whereas *PCSK9* gene knockdown (via PCSK9 siRNA, 48 hours) raised LDLR protein levels in enterocytes by 50% (Figure 4B). We next investigated whether mechanisms independent of the LDLR were involved in the PCSK9-mediated increase in enterocyte apoB TRL production. We assessed MTP protein levels (Figure 4C) and MTP lipid transfer activity (Figure 4D) and found that both were significantly enhanced, by 30–40%, in enterocytes by PCSK9 treatment compared with control untreated cells. Conversely, PCSK9 siRNA inhibition in enterocytes (48 hours) significantly lowered MTP protein levels and activity.

Furthermore, we determined enterocyte levels of Niemann-Pick C1 like 1 (NPC1L1), a critical transporter of cholesterol across the intestinal lumen that affects the overall cellular lipid content²¹. Enterocyte NPC1L1 protein levels were increased by PCSK9 treatment whereas PCSK9 siRNA significantly downregulated NPC1L1 levels (Figure 4E).

PCSK9 Affects the TRL Secretion Machinery *In Vivo* in an LDLR Dependent and Independent Fashion

Human PCSK9 expression in mice increases serum cholesterol via both hepatic LDLR reduction and increased TRL secretion⁵. To test the effect of PCSK9 on the intestine *in vivo*, we used transgenic mice expressing PCSK9 in multiple tissues, including the small and large intestine⁵. Intestinal samples from human PCSK9 transgenic (hPCSK9 tg), WT, and murine PCSK9 knockout (mPCSK9^{-/-}) mice were tested for LDLR levels²².

PCSK9 expression significantly reduced LDLR levels in the small intestine (54%), whereas the absence of mPCSK9 increased LDLR levels by nearly 70% (Supplementary Figures 1). In contrast, PCSK9 overexpression or deletion did not affect LDLR levels in the large intestine (Supplementary Figures 2). We also tested the *in vivo* effect of PCSK9 expression on MTP, the rate-limiting enzyme for TRL particle secretion^{20,23} in the presence or absence of LDLR. Expression of human PCSK9 significantly increased MTP mRNA (3.8-fold),

(Figures 5A and 5B) and protein (2-fold), (Figure 5C, lanes 1–3) levels compared with WT mice. In agreement with canonical knowledge that fat absorption and assembly of chylomicrons occurs in the small intestine²⁴, MTP protein was not detected in the large intestine (Figure 5C, lanes 4–6). Human PCSK9 expression resulted in a significant (32%) increase in MTP activity (Figure 5D), but the absence of mPCSK9 did not alter MTP at any level, mRNA, protein or activity.

The LDLR independent effect of PCSK9 on TRL secretion was further tested in mice expressing hPCSK9 but not LDLR. Figures 6A and 6B show that MTP mRNA levels were increased 3.9-fold in LDLR^{-/-} expressing human PCSK9 compared with control LDLR^{-/-} mice, with protein expression also showing a similar trend (Figure 6C). As expected, MTP was not expressed in the large intestine of LDLR^{-/-} mice (Figure 6B). Finally, MTP activity was increased by 37% ($p < 0.05$) in the small intestine of LDLR^{-/-} mice expressing hPCSK9 (Figure 6D).

Discussion

The controversy about whether variations in PCSK9 concentrations affect TRL levels in humans was settled with recent studies showing significant associations between serum PCSK9 levels and the levels of circulating TRL markers in a broad spectrum of the population^{25,26}. In the present study, we have further shown for the first time that physiologic levels of human PCSK9 directly stimulate intestinal TRL apoB48 and apoB100 production by 50%. Given the role that intestinal TRL production in humans play in determining serum lipid levels after a meal^{10,11}, this magnitude of increase in intestinal TRL apoB production by PCSK9 should be a significant contributor to post-prandial lipids. In addition, this level of TRL apoB stimulation can influence fasting triglycerides in conditions of dysregulated hepatic TRL production, characteristic of individuals with insulin resistance and metabolic syndrome^{10,11}. Furthermore, since one apoB molecule is present per TRL particle, this level of increase in TRL apoB by PCSK9 suggests a potential doubling in the levels of pro-atherogenic TRL intestinal remnant particles in the circulation after a meal.

We further characterized the dynamics of PCSK9-induced stimulation of intestinal TRL and found that it was rapid and prolonged, affecting both cellular and secreted apoB levels. More specifically, the enhancement in enterocyte apoB by extracellular PCSK9 was observed as early as 4 hours post-treatment and persisted 24 hours. Furthermore, PCSK9 increased both cellular and secreted apoB protein levels by similar extents, which indicates that the apoB synthesized in the enterocyte in response to PCSK9 induction is stable and preserved throughout the secretory pathway, without significant degradation.

Importantly, we identified for the first time the cellular and molecular mechanisms through which PCSK9 drives intestinal TRL overproduction. First, we showed that PCSK9 stimulates enterocyte synthesis of both the major protein and lipid components of TRL particles – apoB and triglycerides – by altering cellular processes at both the transcriptional and post-transcriptional levels. Moreover, the PCSK9-mediated increase in intestinal TRL production *in vitro* and *in vivo* was attributed to both LDLR-dependent and independent

mechanisms, involving both transcriptional effects on apoB, MTP and lipogenic genes and post-transcriptional effects on MTP.

We show here that a portion of the PCSK9 that enters the cell from the extracellular compartment remains intact, does not undergo lysosomal degradation and is able to alter intracellular processes. This may explain how extracellular PCSK9 selectively activates transcriptional and post-transcriptional processes. The observation that a portion of internalized PCSK9 is not degraded has been recently reported by us after finding human PCSK9 in liver of mice 4 hours after injection of exogenous human PCSK9⁵. Similarly, a recent study with human fibroblasts has documented that a portion of internalized PCSK9 is diverted from the lysosomal degradation pathway to endocytic recycling compartments²⁷. It is unclear whether this mechanism involves dissociation of PCSK9 from LDLR or if it is a route for the coupled recycling for both protein partners.

At the transcriptional level, PCSK9 caused a significant increase in enterocyte apoB mRNA levels, an effect not observed with apoB regulators such as insulin and fatty acids²⁸. Indeed, prior studies had suggested that apoB is solely regulated post-transcriptionally²⁰. In contrast, here, we demonstrate a strong transcriptional effect of PCSK9 on apoB.

Processes involved in post-transcriptional apoB stability and degradation were also enhanced by PCSK9. Since intracellular neutral lipids inhibit apoB protein degradation and enhance apoB protein stability^{16,20}, the increase in enterocyte neutral lipid content that we observed with PCSK9 treatment explains in part the PCSK9-mediated increase in cellular apoB. An increase in *de novo* cellular triglyceride biosynthesis by PCSK9 can account for this increase in enterocyte neutral lipids, as PCSK9 stimulated the expression of target genes in the *SREBP1* fatty acid/triglyceride biosynthesis pathway (*FAS*, *SCD* and *DGAT2*). PCSK9, however, did not alter the expression of genes in the *SREBP2* cholesterol biosynthesis/uptake pathway.

While *de novo* cellular cholesterol biosynthesis mediated by *SREBP2* was not enhanced by PCSK9, PCSK9, nonetheless, increased cellular levels of NPC1L1 (by 30–40%), critical in mediating intestinal cholesterol transport, absorption, and incorporation into enterocytes²⁹. With respect to potential mechanisms through which PCSK9 might have increased NPC1L1 protein levels, NPC1L1 levels are regulated by both transcription factors, *SREBP2* and PPAR alpha³⁰ PPAR alpha in turn is activated *FAS*³¹. Since PCSK9 treatment significantly increased *FAS* mRNA expression, PPAR alpha mediated upregulation of NPC1L1 is the likely mechanism by which PCSK9 increased enterocyte NPC1L1 protein and will specifically need to be tested in future studies.

MTP, an ER apoB chaperone critical for the transfer of lipids to apoB²³, also contributed to the enhanced apoB stability induced by PCSK9. PCSK9 treatment significantly increased MTP mRNA, protein and lipid transfer activity. The PCSK9-mediated 30–40% increase in MTP activity occurred rapidly, within 24 hours, for a protein whose half-life is four days³². Such a rapid effect can be explained by a stimulatory effect on the *de novo* MTP protein synthesis.

In addition to the above LDLR-independent regulators of apoB production, the LDLR is well known to affect hepatic apoB stability²². PCSK9 also influences intestinal apoB production by reducing enterocyte LDLR levels *in vitro* by 50%.

In vivo human PCSK9 overexpression reduced LDLR levels and increased MTP expression and activity in the small intestine, both known to affect TRL secretion rates^{17,22}. The increased MTP levels and activity persisted in the absence of LDLR in mice expressing human PCSK9. Surprisingly, deletion of PCSK9 in mice did not significantly affect either MTP expression or activity, suggesting a specific effect of human PCSK9, and demonstrating the human relevance of our findings. In fact, neither deletion nor transgenic expression of murine PCSK9 affect cholesterol levels in mice lacking the LDLR³, whereas transgenic expression of human PCSK9 increases serum TRL and TRL secretion in LDLR^{-/-} mice⁵. An important implication of these prior studies, combined with our *in vivo* results above, is that human and murine PCSK9 appear to behave differently in the absence of the LDLR.

Of note, acute siRNA-induced inhibition of *PCSK9* gene expression markedly reduced (by 50%) intestinal TRL apoB cellular protein and mRNA levels and down-regulated production of several enzymes involved in the enterocyte TRL synthesis and assembly process – MTP, NPC1L1 and cholesterol biosynthetic enzymes. The decline in the expression of multiple cholesterol biosynthetic enzymes in the cellular SREBP2 pathway that we observed was an unanticipated benefit of PCSK9 inhibition. PCSK9 knockdown also raised enterocyte LDLR levels by 50%, a significant albeit lesser effect than what we observed in hepatocytes¹⁵. These results further highlight the key role of PCSK9 as an essential regulator of intestinal TRL production.

As a side effect, PCSK9 siRNA treatment of enterocytes also resulted in a very mild increase in cellular neutral lipid content. This is probably attributable to the counter-regulator effect of PCSK9 siRNA in inducing a small increase in DGAT2 mRNA levels, as a result of SREBP1 activation.

In the context of the rapid development and success to date of PCSK9 as a drug target³³, it is critical to unravel the pleiotropic effects of PCSK9 on lipoprotein metabolism. Our results suggest that in addition to its established role as a mediator of hepatic LDL metabolism, PCSK9 is an essential regulator of intestinal TRL metabolism. Thus, our findings prove that the targeted effects of PCSK9 in mediating cellular lipid and lipoprotein metabolism are broad and not limited to the LDLR apoB degrading action of PCSK9, as was initially thought. Moreover, the results demonstrate the potential of PCSK9 as a highly attractive therapeutic drug target also for mitigating TRL production.

While the current studies were focused on the intestine, the potential for PCSK9 TRL-based therapies that we showed here likely also extends beyond the intestine to hepatic TRL metabolism, since parallel TRL pathways are present in hepatocytes. Consistent with this notion, we recently showed that human PCSK9 expression also increases hepatic secretion of TRL in an LDLR-independent fashion in mice⁵. A further potentially important advantage of PCSK9-based TRL therapies, in comparison to the currently available MTP

inhibitor therapies, which also specifically target the TRL apoB production pathway, is that they appear in our studies to lead to less cellular lipid accumulation and may, thus, avoid the unavoidable risk of steatosis seen with MTP inhibitors²³. Indeed, while abetalipoproteinemia patients with loss-of-function mutations in *MTP* demonstrate steatotic effects³⁴, individuals with loss-of-function mutations in *PCSK9* show an absence in hepatic lipid accumulation and steatosis³⁵. Overall, the future of PCSK9-based therapies hold great promise in overcoming long held challenge in developing clinically effective and safe atherosclerotic cardiovascular disease reducing therapies for mitigating hypertriglyceridemia in humans.

Supplementary Material

Refer to Web version on PubMed Central for supplementary material.

Acknowledgments

Funding Sources: This study was partially supported by Merck and Co. through a research grant to Shirya Rashid, and by the National Institutes of Health (NHLBI) through grant R01-HL106845 to Sergio Fazio.

References

1. Abifadel M, Varret M, Rabes JP, Allard D, Ouguerram K, Devillers M, Cruaud C, Benjannet S, Wickham L, Erlich D, Derre A, Villeger L, Farnier M, Beucler I, Bruckert E, Chambaz J, Chanu B, Lecerf JM, Luc G, Moulin P, Weissenbach J, Prat A, Krempf M, Junien C, Seidah NG, Boileau C. Mutations in PCSK9 cause autosomal dominant hypercholesterolemia. *Nat Genet.* 2003; 34:154–156. [PubMed: 12730697]
2. Cohen JC, Boerwinkle E, Mosley TH Jr, Hobbs HH. Sequence variations in PCSK9, low LDL, and protection against coronary heart disease. *N Engl J Med.* 2006; 354:1264–1272. [PubMed: 16554528]
3. Denis M, Marcinkiewicz J, Zaid A, Gauthier D, Poirier S, Lazure C, Seidah NG, Prat A. Gene inactivation of proprotein convertase subtilisin/kexin type 9 reduces atherosclerosis in mice. *Circulation.* 2012; 125:894–901. [PubMed: 22261195]
4. Rashid S, Curtis DE, Garuti R, Anderson NN, Bashmakov Y, Ho YK, Hammer RE, Moon YA, Horton JD. Decreased plasma cholesterol and hypersensitivity to statins in mice lacking Pcsk9. *Proc Natl Acad Sci U S A.* 2005; 102:5374–5379. [PubMed: 15805190]
5. Tavori H, Fan D, Blakemore JL, Yancey PG, Ding L, Linton MF, Fazio S. Serum proprotein convertase subtilisin/kexin type 9 and cell surface low-density lipoprotein receptor: evidence for a reciprocal regulation. *Circulation.* 2013; 127:2403–2413. [PubMed: 23690465]
6. Ouguerram K, Chetiveaux M, Zair Y, Costet P, Abifadel M, Varret M, Boileau C, Magot T, Krempf M. Apolipoprotein B100 metabolism in autosomal-dominant hypercholesterolemia related to mutations in PCSK9. *Arterioscler Thromb Vasc Biol.* 2004; 24:1448–1453. [PubMed: 15166014]
7. Boekholdt SM, Arsenault BJ, Mora S, Pedersen TR, LaRosa JC, Nestel PJ, Simes RJ, Durrington P, Hitman GA, Welch KM, DeMicco DA, Zwiderman AH, Clearfield MB, Downs JR, Tonkin AM, Colhoun HM, Gotto AM Jr, Ridker PM, Kastelein JJ. Association of LDL cholesterol, non-HDL cholesterol, and apolipoprotein B levels with risk of cardiovascular events among patients treated with statins: a meta-analysis. *JAMA.* 2012; 307:1302–1309. [PubMed: 22453571]
8. Chapman MJ, Ginsberg HN, Amarengo P, Andreotti F, Boren J, Catapano AL, Descamps OS, Fisher E, Kovanen PT, Kuivenhoven JA, Lesnik P, Masana L, Nordestgaard BG, Ray KK, Reiner Z, Taskinen MR, Tokgozoglul L, Tybjaerg-Hansen A, Watts GF. Triglyceride-rich lipoproteins and high-density lipoprotein cholesterol in patients at high risk of cardiovascular disease: evidence and guidance for management. *Eur Heart J.* 2011; 32:1345–1361. [PubMed: 21531743]

9. Sun H, Samarghandi A, Zhang N, Yao Z, Xiong M, Teng BB. Proprotein convertase subtilisin/kexin type 9 interacts with apolipoprotein B and prevents its intracellular degradation, irrespective of the low-density lipoprotein receptor. *Arterioscler Thromb Vasc Biol.* 2012; 32:1585–1595. [PubMed: 22580899]
10. Shojaee-Moradie F, Ma Y, Lou S, Hovorka R, Umpleby AM. Prandial Hypertriglyceridemia in Metabolic Syndrome is due to an Overproduction of both Chylomicron and VLDL Triacylglycerol. *Diabetes.* 2013; 62:4063–4069. [PubMed: 23990358]
11. Adeli K, Lewis GF. Intestinal lipoprotein overproduction in insulin-resistant states. *Curr Opin Lipidol.* 2008; 19:221–228. [PubMed: 18460911]
12. Seidah NG, Benjannet S, Wickham L, Marcinkiewicz J, Jasmin SB, Stifani S, Basak A, Prat A, Chretien M. The secretory proprotein convertase neural apoptosis-regulated convertase 1 (NARC-1): liver regeneration and neuronal differentiation. *Proc Natl Acad Sci U S A.* 2003; 100:928–933. [PubMed: 12552133]
13. Qian YW, Schmidt RJ, Zhang Y, Chu S, Lin A, Wang H, Wang X, Beyer TP, Bensch WR, Li W, Ehsani ME, Lu D, Konrad RJ, Eacho PI, Moller DE, Karathanasis SK, Cao G. Secreted PCSK9 downregulates low density lipoprotein receptor through receptor-mediated endocytosis. *J Lipid Res.* 2007; 48:1488–1498. [PubMed: 17449864]
14. Fan D, Yancey PG, Qiu S, Ding L, Weeber EJ, Linton MF, Fazio S. Self-association of human PCSK9 correlates with its LDLR-degrading activity. *Biochemistry.* 2008; 47:1631–1639. [PubMed: 18197702]
15. Melone M, Wilsie L, Palyha O, Strack A, Rashid S. Discovery of a new role of human resistin in hepatocyte low-density lipoprotein receptor suppression mediated in part by proprotein convertase subtilisin/kexin type 9. *J Am Coll Cardiol.* 2012; 59:1697–1705. [PubMed: 22554600]
16. Costandi J, Melone M, Zhao A, Rashid S. Human resistin stimulates hepatic overproduction of atherogenic ApoB-containing lipoprotein particles by enhancing ApoB stability and impairing intracellular insulin signaling. *Circ Res.* 2011; 108:727–742. [PubMed: 21293001]
17. Athar H, Iqbal J, Jiang XC, Hussain MM. A simple, rapid, and sensitive fluorescence assay for microsomal triglyceride transfer protein. *J Lipid Res.* 2004; 45:764–772. [PubMed: 14754905]
18. Lambert G, Ancellin N, Charlton F, Comas D, Pilot J, Keech A, Patel S, Sullivan DR, Cohn JS, Rye KA, Barter PJ. Plasma PCSK9 concentrations correlate with LDL and total cholesterol in diabetic patients and are decreased by fenofibrate treatment. *Clin Chem.* 2008; 54:1038–1045. [PubMed: 18436719]
19. Traber MG, Kayden HJ, Rindler MJ. Polarized secretion of newly synthesized lipoproteins by the Caco-2 human intestinal cell line. *J Lipid Res.* 1987; 28:1350–1363. [PubMed: 3430064]
20. Adeli K, Taghibiglou C, Van Iderstine SC, Lewis GF. Mechanisms of hepatic very low-density lipoprotein overproduction in insulin resistance. *Trends Cardiovasc Med.* 2001; 11:170–176. [PubMed: 11597827]
21. Garcia-Calvo M, Lisnock J, Bull HG, Hawes BE, Burnett DA, Braun MP, Crona JH, Davis HR Jr, Dean DC, Detmers PA, Graziano MP, Hughes M, Macintyre DE, Ogawa A, O'neill KA, Iyer SP, Shevell DE, Smith MM, Tang YS, Makarewicz AM, Ujjainwalla F, Altmann SW, Chapman KT, Thornberry NA. The target of ezetimibe is Niemann-Pick C1-Like 1 (NPC1L1). *Proc Natl Acad Sci U S A.* 2005; 102:8132–8137. [PubMed: 15928087]
22. Gillian-Daniel DL, Bates PW, Tebon A, Attie AD. Endoplasmic reticulum localization of the low density lipoprotein receptor mediates presecretory degradation of apolipoprotein B. *Proc Natl Acad Sci U S A.* 2002; 99:4337–4342. [PubMed: 11904390]
23. Cuchel M, Rader DJ. Microsomal transfer protein inhibition in humans. *Curr Opin Lipidol.* 2013; 24:246–250. [PubMed: 23594709]
24. Swift LL, Jovanovska A, Kakkad B, Ong DE. Microsomal triglyceride transfer protein expression in mouse intestine. *Histochem Cell Biol.* 2005; 123:475–482. [PubMed: 15891896]
25. Lakoski SG, Lagace TA, Cohen JC, Horton JD, Hobbs HH. Genetic and metabolic determinants of plasma PCSK9 levels. *J Clin Endocrinol Metab.* 2009; 94:2537–2543. [PubMed: 19351729]
26. Baass A, Dubuc G, Tremblay M, Delvin EE, O'Loughlin J, Levy E, Davignon J, Lambert M. Plasma PCSK9 is associated with age, sex, and multiple metabolic markers in a population-based sample of children and adolescents. *Clin Chem.* 2009; 55:1637–1645. [PubMed: 19628659]

27. Nguyen MA, Kosenko T, Lagace TA. Internalized PCSK9 dissociates from recycling LDL receptors in PCSK9-resistant SV-589 fibroblasts. *J Lipid Res.* 2014; 55:266–275. [PubMed: 24296664]
28. Dashti N, Williams DL, Alaupovic P. Effects of oleate and insulin on the production rates and cellular mRNA concentrations of apolipoproteins in HepG2 cells. *J Lipid Res.* 1989; 30:1365–1373. [PubMed: 2689548]
29. Zhang JH, Ge L, Qi W, Zhang L, Miao HH, Li BL, Yang M, Song BL. The N-terminal domain of NPC1L1 protein binds cholesterol and plays essential roles in cholesterol uptake. *J Biol Chem.* 2011; 286:25088–25097. [PubMed: 21602275]
30. Yu L. The structure and function of Niemann-Pick C1-like 1 protein. *Curr Opin Lipidol.* 2008; 19:263–269. [PubMed: 18460917]
31. Jensen-Urstad AP, Semenkovich CF. Fatty acid synthase and liver triglyceride metabolism: housekeeper or messenger? *Biochim Biophys Acta.* 2012; 1821:747–753. [PubMed: 22009142]
32. Lin MC, Gordon D, Wetterau JR. Microsomal triglyceride transfer protein (MTP) regulation in HepG2 cells: insulin negatively regulates MTP gene expression. *J Lipid Res.* 1995; 36:1073–1081. [PubMed: 7658155]
33. King A. Lipids. Antibodies against PCSK9--a new era of therapy. *Nat Rev Cardiol.* 2013; 10:1. [PubMed: 23165073]
34. Bernard S, Touzet S, Personne I, Lapras V, Bondon PJ, Berthezene F, Moulin P. Association between microsomal triglyceride transfer protein gene polymorphism and the biological features of liver steatosis in patients with type II diabetes. *Diabetologia.* 2000; 43:995–999. [PubMed: 10990076]
35. Duff CJ, Hooper NM. PCSK9: an emerging target for treatment of hypercholesterolemia. *Expert Opin Ther Targets.* 2011; 15:157–168. [PubMed: 21204732]

Figure 1A.

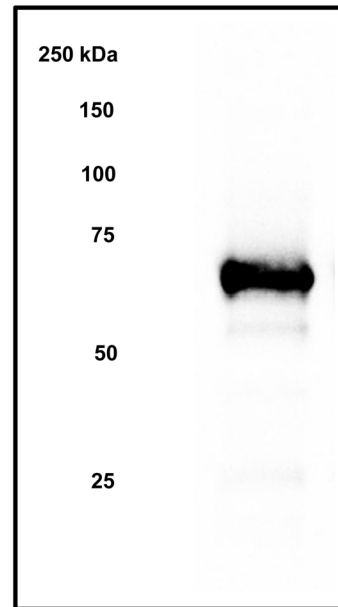


Figure 1B.

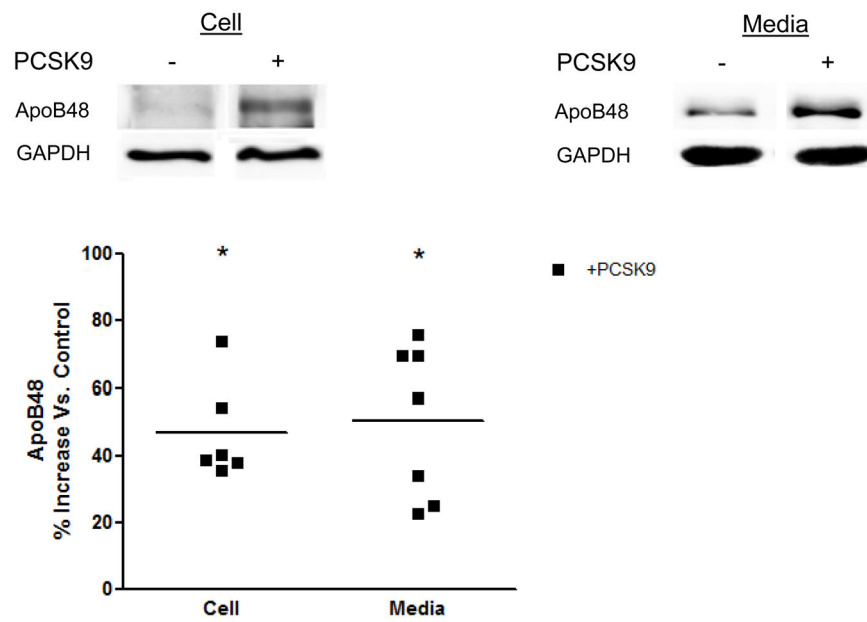


Figure 1C.

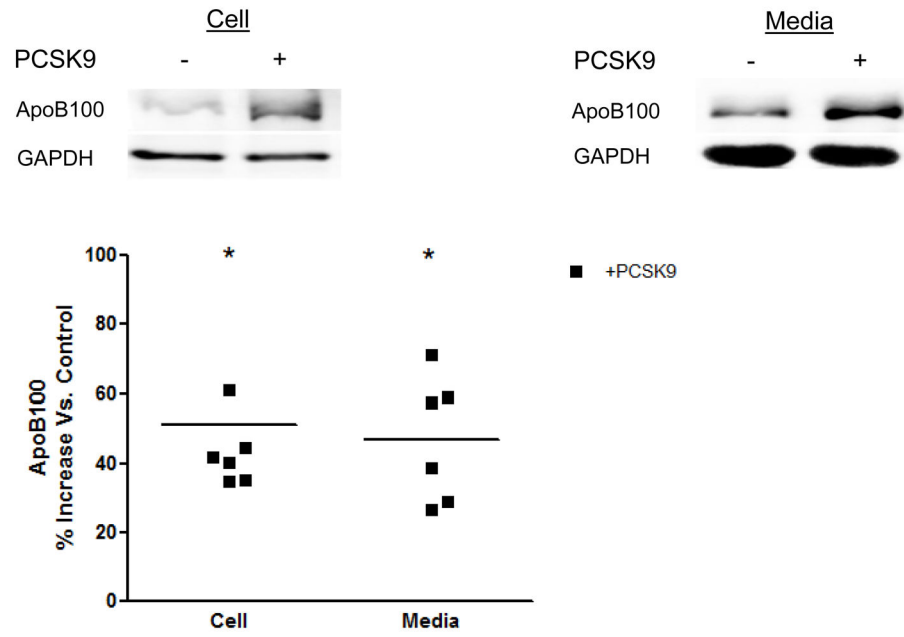


Figure 1D.

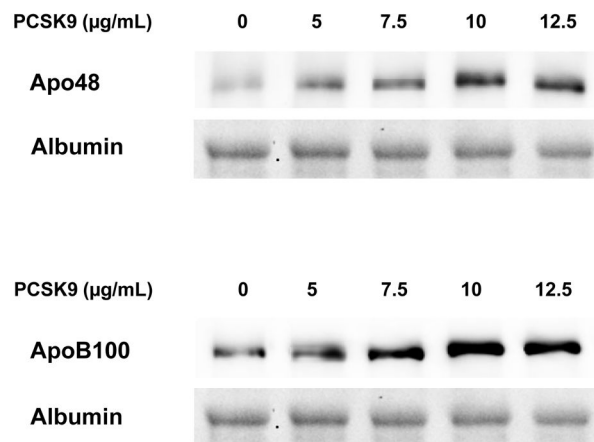


Figure 1E.

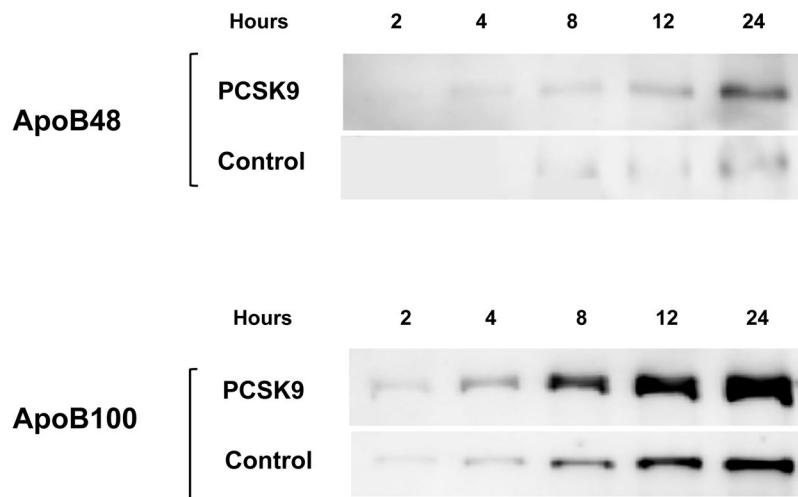


Figure 1.

Direct Stimulatory Effect of PCSK9 on ApoB Expression and Secretion in Human Enterocytes. (A) The human recombinant human PCSK9 used in all experiments was characterized via immunoblotting. A 2 µg quantity of recombinant human PCSK9 was immunoblotted using 10% SDS gels and a polyclonal antibody against human PCSK9. The results confirmed the expected 62 kDa size of recombinant human PCSK9. (B) PCSK9 treatment (10 µg/mL, 24 hours) significantly stimulated the cellular expression and secretion of apoB48 protein (by 40–50%) in optimally polarized CaCo-2 cells, compared with control untreated cells, maintained in 1% FBS. (C) PCSK9 (10 µg/mL, 24 hours) markedly stimulated the cellular expression and secretion of apoB100 protein (by 40–50%) in CaCo-2 cells, compared with control untreated cells, maintained in 1% FBS. (D) The stimulatory effect of PCSK9 (24 hours) on apoB48 and apoB100 secretion in CaCo-2 cells (compared with control untreated cells maintained in 1% FBS) occurred in a dose-responsive manner in the 0 to 12.5 µg/mL concentration range of PCSK9. The maximum stimulatory effect was reached at 10 µg/mL PCSK9. (E) Time course effects of PCSK9 treated CaCo-2 cells (10 µg/mL) showed an enhancement in both apoB48 and apoB100 secretion as early as 4 hours post-treatment (versus control untreated cells) and continued on to the 24-hour time-frame of the study.

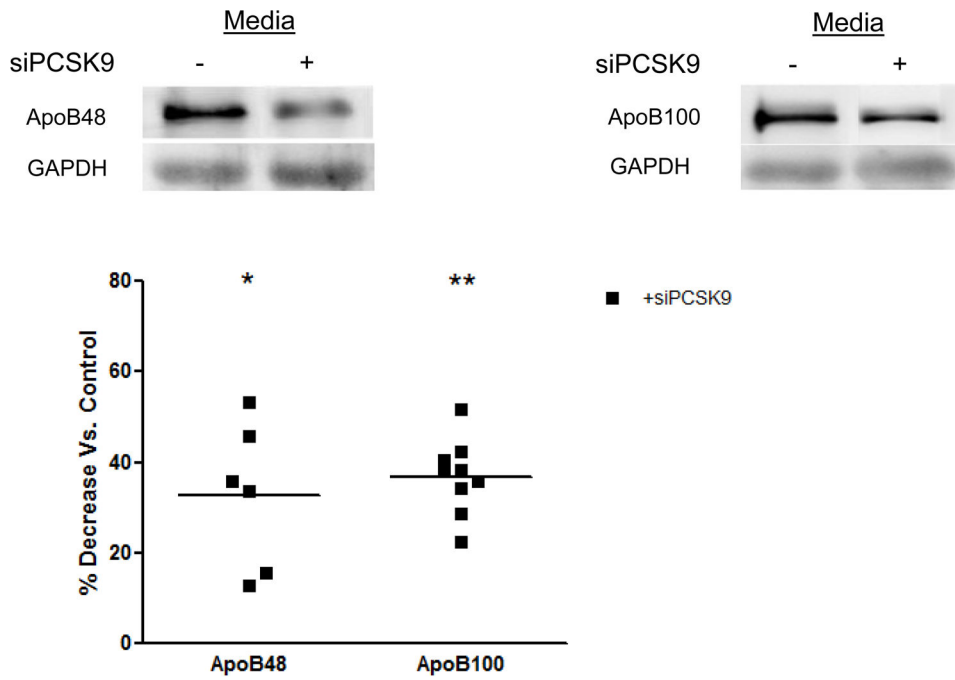


Figure 2. Inhibition of Enterocyte ApoB Secretion by Acute Deletion of *PCSK9* Gene Expression. CaCo-2 cells treated with PCSK9 siRNA (15 nmol/L, 48 hours) showed a 70% reduction in PCSK9 mRNA expression versus CaCo-2 cells transfected with a negative control vector, and demonstrated no significant decline in cellular viability versus untreated cells (results not shown). PCSK9 siRNA knockdown resulted in a nearly 40% decrease in both apoB48 and apoB100 secretion from CaCo-2 cells.

Figure 3A.

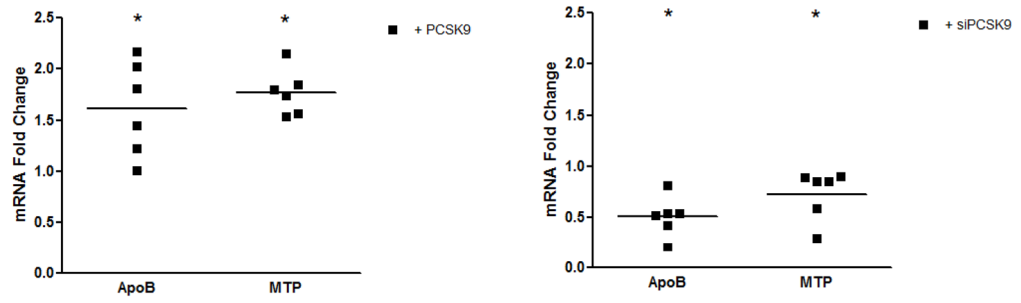


Figure 3B.

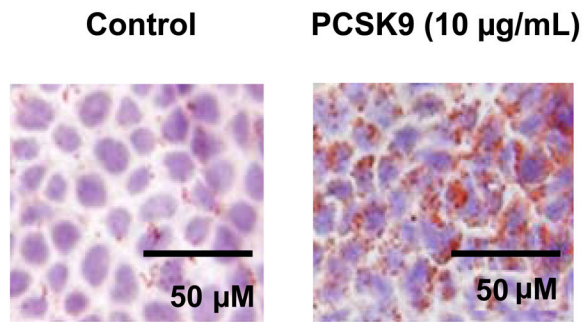


Figure 3C.

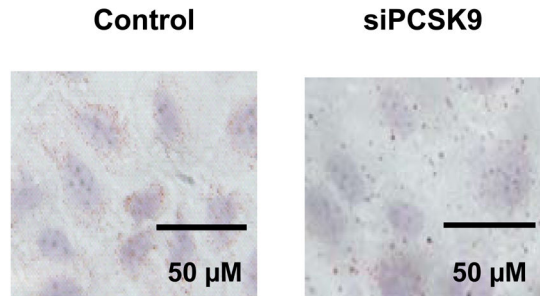


Figure 3D.

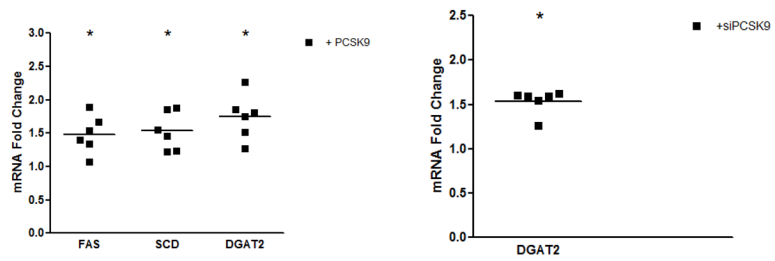


Figure 3E.

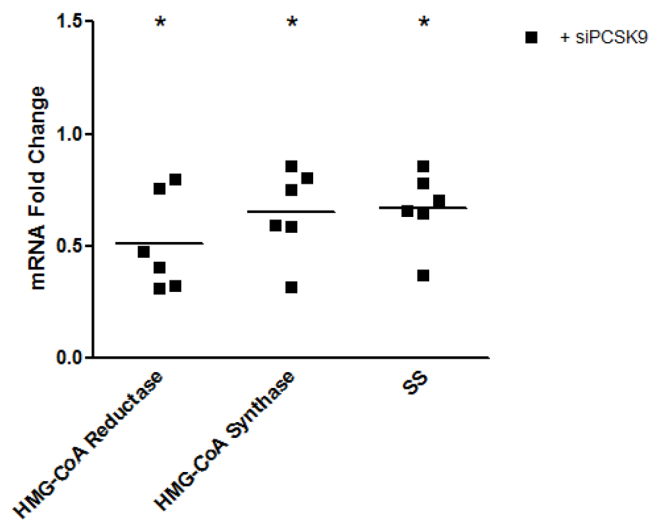


Figure 3.

PCSK9-Induced Changes in Expression Levels of Genes Involved in the Control of Enterocyte Lipid and Lipoprotein Biosynthesis. (A) The mRNA levels of *APOB* and *MTP* genes were assessed by real-time RT-PCR in CaCo-2 cells treated with 10 µg/mL PCSK9 for 24 hours and in cells transfected with PCSK9 siRNA for 48 hours and compared to control cells. PCSK9 treatment resulted in a significant 1.5 fold increase in cellular apoB mRNA content versus untreated control cells. PCSK9 also caused a similar 1.5 increase in cellular MTP mRNA content. PCSK9 siRNA treatment resulted in a significant 50% decline in cellular apoB mRNA content versus control cells treated with a scrambled siRNA control vector. PCSK9 also caused a 20% decrease in cellular MTP mRNA content. (B) The lipid content of CaCo-2 cells treated with PCSK9 (10 µg/mL, 24 hours) was assessed using Oil-Red-O/hematoxylin staining. PCSK9 treated CaCo-2 showed a markedly greater cellular neutral lipid content (triglycerides and cholesteryl esters) than untreated control cells. (C) The lipid content of CaCo-2 cells treated with PCSK9 siRNA (48 hours) was assessed using Oil-Red-O/hematoxylin staining. CaCo-2 cells treated with PCSK9 siRNA showed a slightly elevated neutral lipid content (triglycerides and cholesteryl esters) compared to control cells treated with a scrambled siRNA control vector. (D) The mRNA levels of target genes in the SREBP1 intracellular lipid biosynthesis pathway were assessed in CaCo-2 cells treated with PCSK9 (10 µg/mL, 24 hours) and in cells transfected with PCSK9 siRNA (48 hours), via real-time RT-PCR. The mRNA levels of target genes in the SREBP1 pathway involved in cellular fatty acid biosynthesis (*FAS* and *SCD*) and triglyceride biosynthesis (*DGAT2*) were significantly greater in enterocytes treated with PCSK9 than in control untreated cells. *DGAT2* mRNA levels but not other SREBP1 target genes, were slightly higher in PCSK9 siRNA transfected enterocytes compared with control cells treated with a scrambled siRNA control vector. (E) The mRNA levels of target genes in the SREBP2 cholesterol biosynthesis pathway were assessed in CaCo-2 cells treated with PCSK9 siRNA (48 hours) via real-time RT-PCR. The mRNA levels of *HGMCR*, *HMGCS* and *SS*, but not other SREBP2 target genes, were significantly reduced in PCSK9 siRNA transfected enterocytes compared with control cells treated with a scrambled siRNA control vector.

Figure 4A.

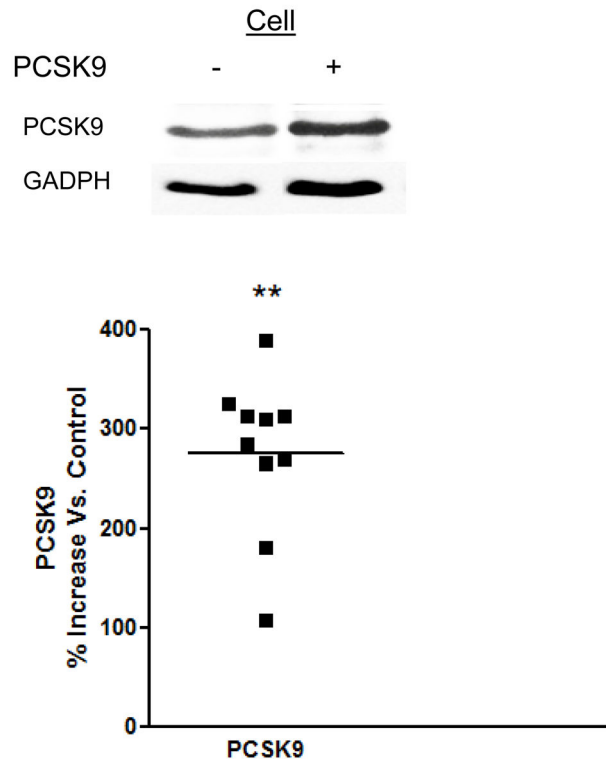


Figure 4B.

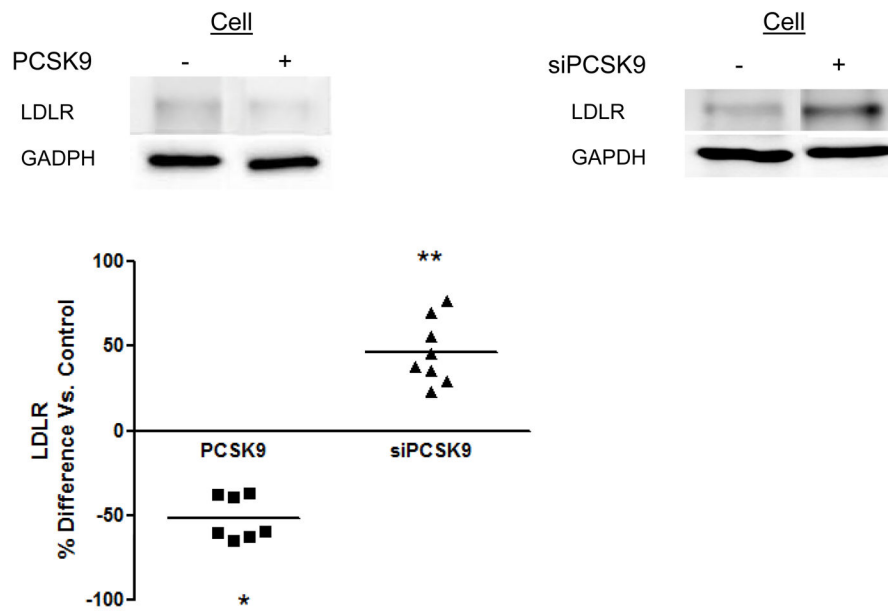


Figure 4C.

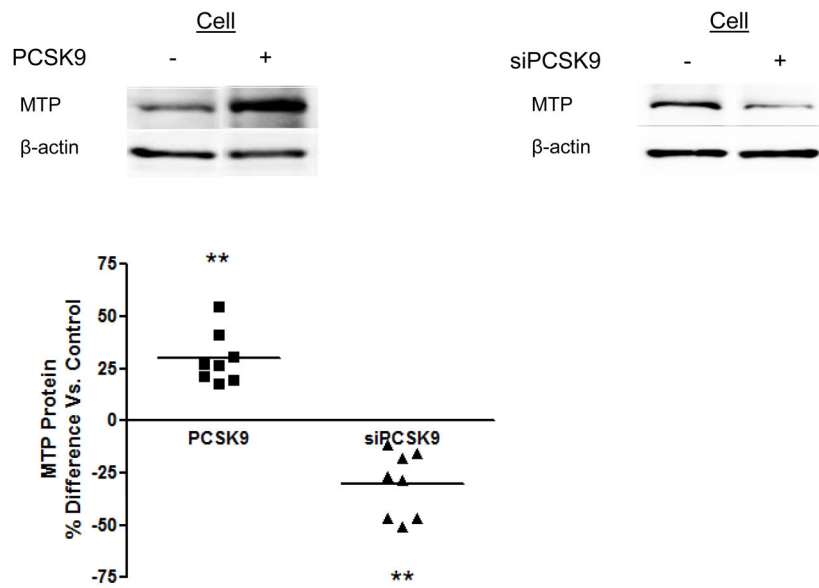


Figure 4D.

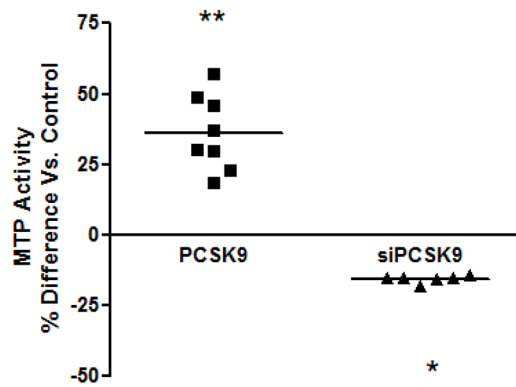


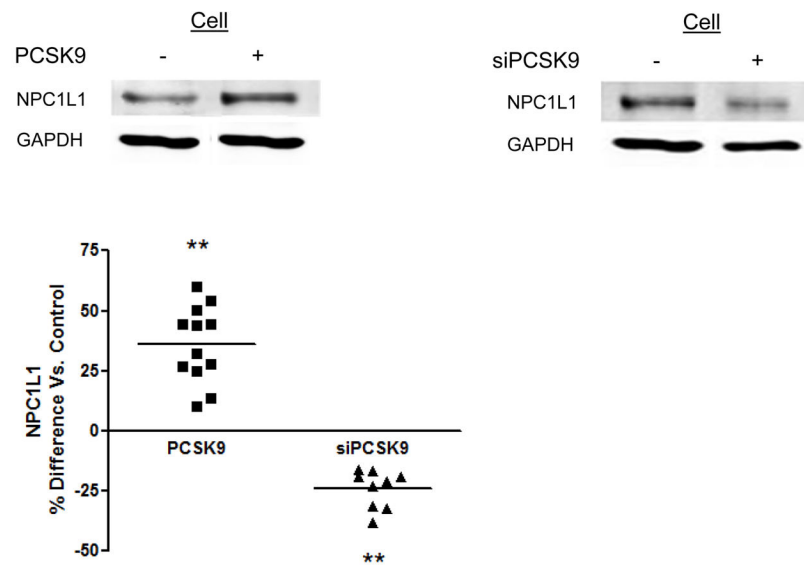
Figure 4E.

Figure 4. Protein Mediators of the Cellular TRL Production Process Accounting for Alterations in Enterocyte ApoB Induced by PCSK9. (A) CaCo-2 cells treated with PCSK9 (10 $\mu\text{g}/\text{mL}$, 24 hours) showed a significant 250% (2.5-fold) increase in cellular PCSK9 protein levels versus control untreated cells. (B) CaCo-2 cells treated with PCSK9 (10 $\mu\text{g}/\text{mL}$, 24 hours) showed a significant 50% reduction in LDLR protein levels versus control untreated cells. Conversely, siRNA *PCSK9* gene knockdown (15 nmol/L, 48 hours) resulted in a nearly 50% increase in LDLR protein. (C) PCSK9 (10 $\mu\text{g}/\text{mL}$, 24 hours) treatment caused a significant 30% increase in CaCo-2 MTP protein levels, whereas siRNA *PCSK9* knockdown (48 hours) caused a 30% reduction in cellular MTP protein. (D) PCSK9 (10 $\mu\text{g}/\text{mL}$, 24 hours) caused a nearly 40% significant increase in MTP activity in CaCo-2 cells. In contrast, siRNA *PCSK9* knockdown (48 hours) resulted a 10% reduction in cellular MTP activity. (E) PCSK9 (10 $\mu\text{g}/\text{mL}$, 24 hours) caused a close to 40% significant increase in CaCo-2 NPC1L1 protein levels, whereas siRNA *PCSK9* knockdown (48 hours) caused a 25% reduction in cellular NPC1L1 protein.

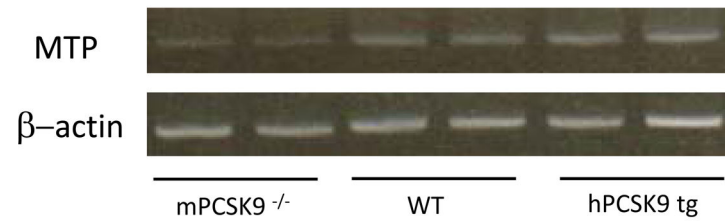
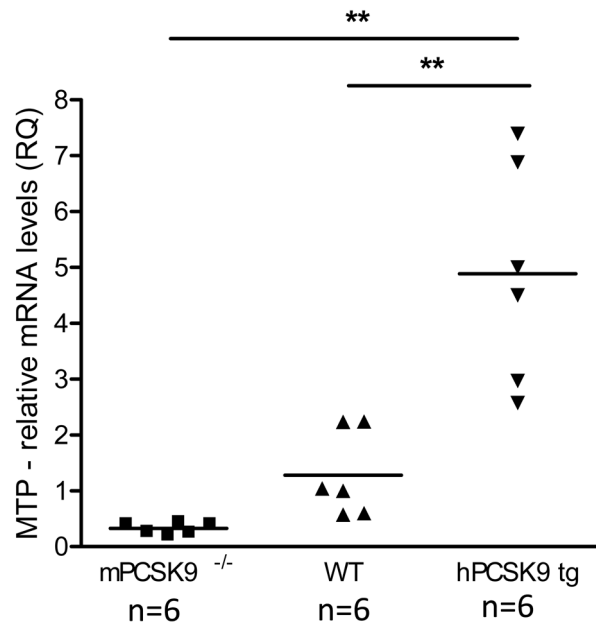
Figure 5A.**Figure 5B.**

Figure 5C.

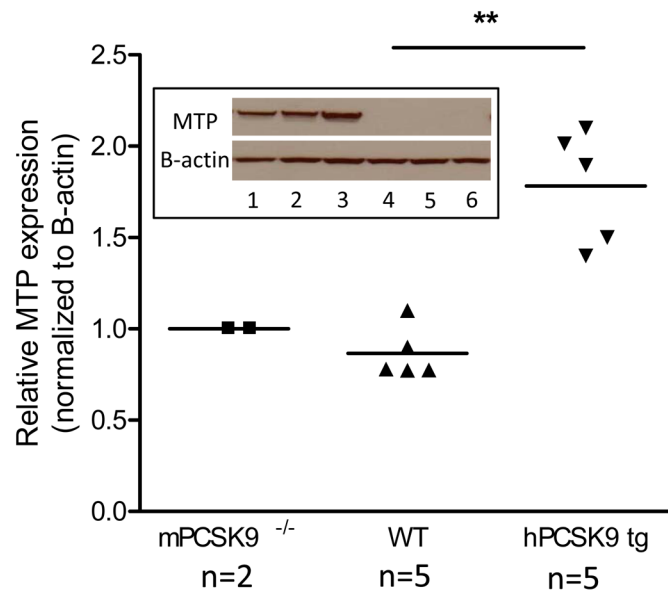


Figure 5D.

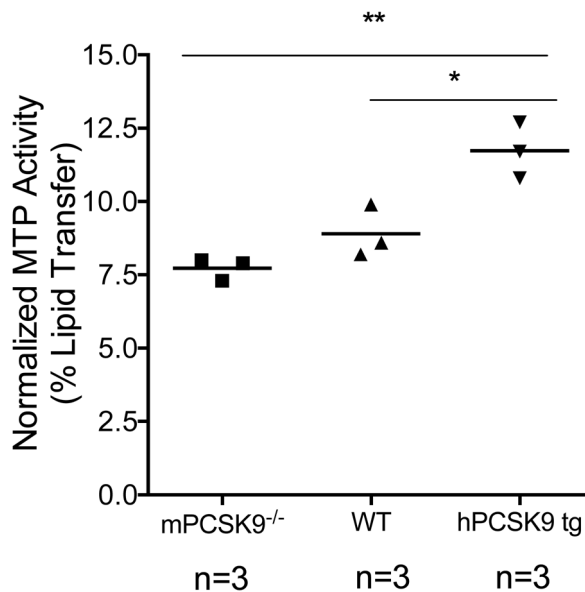


Figure 5.

MTP Levels and Activity in the Small Intestine in mPCSK9 ^{-/-}, WT and hPCSK9 tg Mice. (A) Semi-quantitative PCR results showing mRNA levels of MTP and β -actin in the small intestine. (B) Relative mRNA expression of MTP evaluated by real time RT-PCR.

Expression levels were calculated using the Δ CT method. Each sample was measured in duplicate using 6 mice in each group (n=6) and normalized to 18S rRNA Levels. (C) Quantitative analysis of MTP protein levels normalized to β -actin in the small intestine, with the indicated number of mice. Insert: representative immunoblot of MTP and β -actin in the small and large intestine. Lane 1: mPCSK9 ^{-/-} small intestine; lane 2: WT small intestine; lane 3: hPCSK9 tg small intestine; lane 4: mPCSK9 ^{-/-} large intestine; lane 5: WT large intestine; lane 6: hPCSK9 tg large intestine. (D) MTP activity in the small intestine. MTP activity was measured in duplicate using 3 mice in each group (n=3) and normalized to total protein content. (One-Way ANOVA: *p<0.05, ** p<0.01).

Figure 6A.

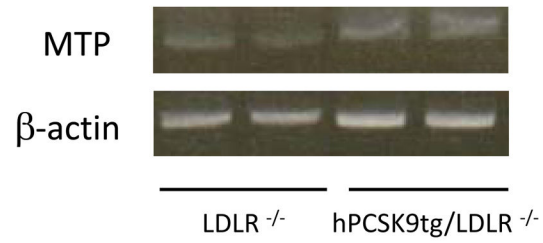


Figure 6B.

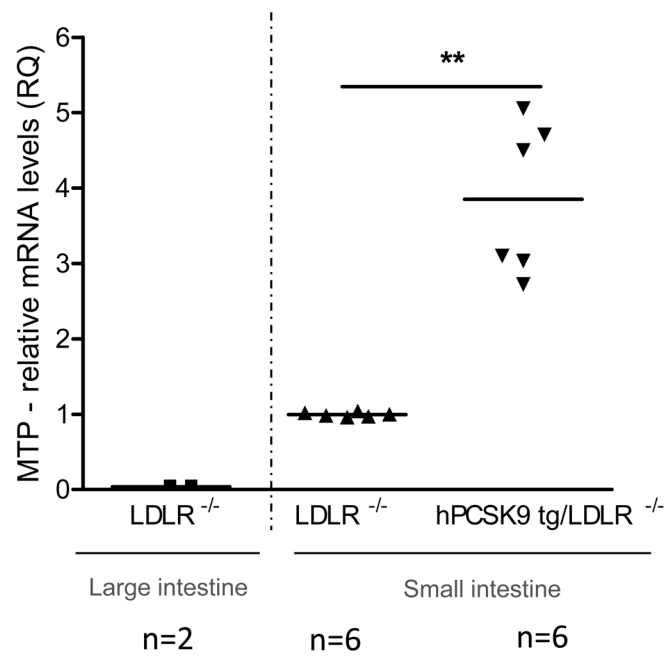


Figure 6C.

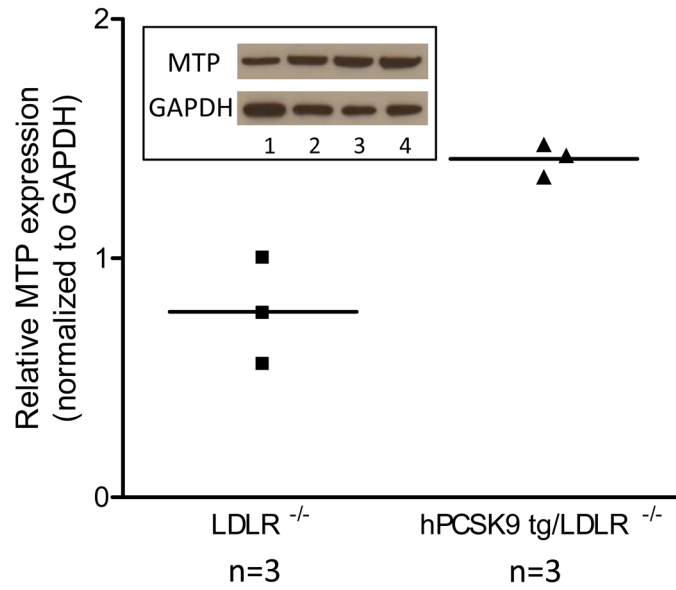


Figure 6D.

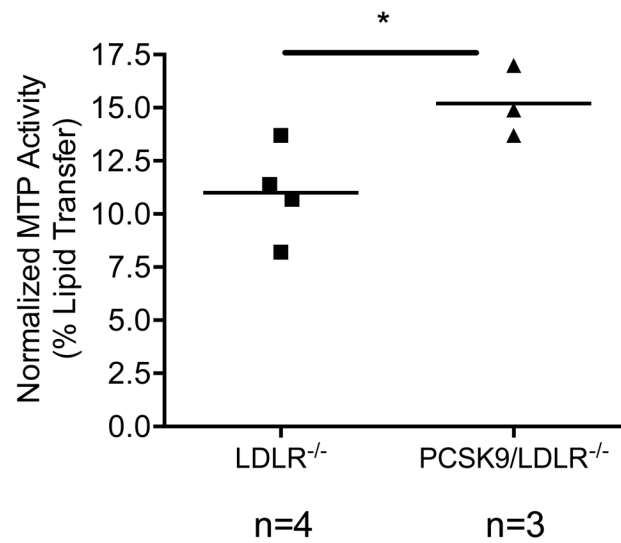


Figure 6.

MTP Levels and Activity in the Small Intestine of WT and hPCSK9 tg Mice on an LDLR $-/-$ background. (A) Semi-quantitative PCR showing mRNA levels of MTP and β -actin in the small intestine. (B) Relative mRNA expression of MTP in the large (LI) and small intestine (SI) evaluated by real time RT-PCR. Expression levels were calculated using the 2^{-CT} method. Each sample was measured in duplicate using the indicated number of mice, and mRNA levels were normalized to 18S rRNA Levels. (C) Quantitative analysis of MTP protein levels normalized to GAPDH in the small intestine (n=3). Insert: representative immunoblot of MTP and GAPDH in the small intestine. Lanes 1, 2: LDLR $-/-$; lanes 3, 4: hPCSK9 tg/LDLR $-/-$. (D) MTP activity in the small intestine. MTP activity was measured in duplicate using the indicated number of mice in each group and normalized to total protein content. (T-test: *p<0.05, ** p<0.01).